

Development of digital bathymetry maps for Lakes Azuei and Enriquillo using sonar and remote sensing techniques

Mahrokh Moknatian¹ | Michael Piasecki¹  | Fred Moshary² | Jorge Gonzalez³

¹Civil Engineering Department, City College of New York, USA

²Electrical Engineering Department, City College of New York, USA

³Mechanical Engineering Department, City College of New York, USA

Correspondence

Michael Piasecki, Civil Engineering Department, City College of New York, 160 Convent Ave, New York 10031, USA.
Email: mpiasecki@ccny.cuny.edu

Funding information

United States National Science Foundation, Grant/Award Number: 1264466 and 1513512

Abstract

This article presents an improved algorithm for optimization and development of a digital bathymetric model (DBM) for Lake Azuei (LA) (Haiti) and Lake Enriquillo (LE) (Dominican Republic) using the ANUDEM method. Both sonar data and contour lines of the lakes' layout extracted using Landsat imagery were compiled for bathymetry development. We show that the performance of the ANUDEM method was strongly dependent on the density and irregularity of the spatial distribution of the data. Changing the resolution of the output grids and deriving auxiliary topographically corrected contours improved the ANUDEM performance and minimized the systematic errors of the method. Statistical analysis showed no significant difference between measured and interpolated depths, characterized by a root mean square error of less than 0.71 m (LE) and 0.96 m (LA), and a median difference of -0.009 m (LE) and 0.012 m (LA) on average. The shape reliability analysis revealed a relationship between accuracy and the depth and slope values, increasing in the center of the lakes where they are deep and the slope is gentle.

This is an open access article under the terms of the Creative Commons Attribution-NonCommercial-NoDerivs License, which permits use and distribution in any medium, provided the original work is properly cited, the use is non-commercial and no modifications or adaptations are made.

© 2019 The Authors. Transactions in GIS Published by John Wiley & Sons Ltd

1 | INTRODUCTION

Digital terrain models (DTMs) representing the gridded surface of features such as ground or reservoir bed/floor are typically derived from interpolation of topographic data. These digital representations of surface elevation and subsurface water body depths are central to many research efforts dealing with water resources, climatology and environmental engineering investigations, and concern for example wind field modeling (Winstral & Marks, 2002), sunlight modeling (Dozier & Frew, 1990), soil erosion estimation (Bhattarai & Dutta, 2007; Lu, Li, Valladares, & Batistella, 2004), sediment movement (Jones, 2002), flood simulation (Bates & De Roo, 2000; Haile & Rientjes, 2005), catchment studies (Vogt, Colombo, & Bertolo, 2003), and limnology (Li, Zhu, & Gold, 2005; Nolan & Brigham-Grette, 2006).

Lake Enriquillo (LE) and Lake Azuei (LA) are located on the island of Hispaniola and have been subject to scientific research interest over the years due to their extensive expanding and shrinking patterns. Recent expansion (starting in 2004) has had significant implications for the region brought on by the inundation of arable land, local highways (impacting the trade routes between Haiti and the Dominican Republic [DR] in the border region), and even requiring the abandonment of villages (Boca de Cachon, DR) and subsequent resettlement. While the lake levels seem to have remained stable over the past 3 years, great interest persists (as attested to by verbal communications with representatives of the Haitian and Dominican Republic governments) in understanding why they grew to these unprecedented levels and subsequently assessing what the future patterns may look like. To this end, a hydrologic analysis is needed that includes the lakes themselves, the watersheds of both lakes, in addition to details of past and future hydroclimato-logical data. Although previous research efforts have used the surface area and/or level fluctuations of the lakes for hydrological studies (Benson & Paillet, 1989; Daut et al., 2010), it is really the volume of the lakes and their rates of change that are needed to formulate a water balance model that could yield a deeper insight into the lake behaviors (Mason, Guzkowska, Rapley, & Street-Perrott, 1994). A necessary step for the volume calculations is thus to obtain a digital representation of not only the surrounding terrain (above lake level), but also the lakes' bathymetry to construct a seamless digital surface (a "bathtub") that includes the lakes' topographical depression and that can be filled/emptied at will.

As the ubiquity of DTM representations has grown over the years, so have different methods of interpolation, namely deterministic interpolation (e.g. inverse distance weighting [IDW] and splines), geostatistical methods (e.g. kriging), and hydrologically correct methods (e.g. the Australian National University Digital Elevation Model [ANUDEM]—Hutchinson, 1989; Hutchinson, Xu, & Stein, 2011 and triangulated irregular networks [TINs]—Arun, 2013; Leon & Cohen, 2012). The accuracy of a generated DTM depends largely on a number of factors including accuracy of data source (Gong, Zhilin, Zhu, Sui, & Zhou, 2000), density of data points (Aguilar, Agüera, Aguilar, & Carvajal, 2005; Chaplot et al., 2006; Gong et al., 2000), spatial and statistical distributions of data points (Gumus & Sen, 2013; Zimmerman, Pavlik, Ruggles, & Armstrong, 1999), the interpolation process itself (Aguilar et al., 2005; Arun, 2013; Gong et al., 2000), type of terrain (Chaplot et al., 2006; Gong et al., 2000; Zimmerman et al., 1999), and finally the required resolution of the output grids (Fisher & Tate, 2006; Kienzle, 2004). Any of these aforementioned factors may introduce errors or inaccuracies in the final product. Moreover, these factors influence the selection of a suitable interpolation method for a specific dataset (Ikechukwu, Ebinne, Idorenyin, & Raphael, 2017). For instance, IDW and spline methods are known to be effective when the density of source data is high and their distribution is homogeneous, because these methods depend largely on the neighborhood of target points (Leon & Cohen, 2012). Tests have shown that IDW yields more accurate results than other methods when generating a DTM from a contour map, which is regularly spaced source data (Tan & Xu, 2014), while splines have been used successfully in cases where the data were more irregularly spaced (Ikechukwu et al., 2017). In contrast, the kriging approach, which is a statistical model, does not require homogeneity of the spatial distribution but requires more steps, such as the normalization of the dataset, and is thus more labor-intensive (Ikechukwu et al., 2017). Another method of generating DTMs is ANUDEM, a hydrological-based interpolation with an underlying iterative finite difference technique (Hutchinson, 1989), similar to the use of splines (Lewis, 2001). This method

was developed for digital topography map generation incorporating drainage features, which makes this method suitable for hydrological and hydroecological analysis (Hutchinson et al., 2011), as evidenced by numerous applications (Parker, Milbert, Wilson, Bailey, & Gesch, 2001; Whiteway, 2009; Yang et al., 2007; Zenger & Wealands, 2004; Zheng, Xiong, Yue, & Gong, 2016). Moreover, this algorithm has also been used for bathymetry generation and many researchers have found it to be an effective tool to produce DBMs for reservoirs (Hradilek, Bašta, Vizina, Máca, & Pech, 2015), lakes (Leon & Cohen, 2012; Popielarczyk & Templin, 2014), coastal areas (Parker et al., 2001; Whiteway, 2009), and seafloor (Daniell, 2008; De Araujo et al., 2016; Fretwell, Tate, Deen, & Belchier, 2009; Hillenbrand, Trathan, Arndt, & Kuhn, 2014). Given that sometimes bathymetry generation for a water body requires special interpolation techniques due to the highly anisotropic distribution of observations as a result of how data were collected (Gold & Condal, 1995), we decided to utilize the ANUDEM method for modeling the LA's and LE's floor. Hydrographic survey data of lakes' depth (Piasecki et al., 2016) and Landsat images were used as inputs for the interpolation process. We derived and optimized the DBMs for both lakes by minimizing the errors of interpolation and removing artifacts created during the interpolation process, employing the void-filling technique suggested by Zheng et al. (2016), which allowed us to also assess the accuracy of volume and depth estimations.

2 | STUDY AREA

LA and LE are situated in close proximity (approximately 3 km apart at their closest point) along a west-to-east orientation and are separated by the Haiti/DR border. LE and LA were formed on marine deposits in the Cul de Sac Depression and feature a fairly rocky and steep shoreline, except on the western and eastern ends where the shoreline exhibits very gentle slopes. LE extends 43 km in the E–W direction and has a width of 15 km N–S, while LA's dimensions are 30 km NW–SE and 10 km NE–SW, making them not only the biggest lakes on the island but also in the entire Caribbean region. The lakes are characterized by a high degree of water-level fluctuations through time. On the north and south, the lakes are bounded by the mountain ranges of Sierra Neiba and Sierra Barahuco, which reach an elevation of more than 2,000 m above sea level. Figure 1 shows the valley and the location of the lakes.

The first bathymetry map available for LE was produced in 1992 (Araguás Araguás, Mchelen, Garcia, Medina, & Febrillet, 1995), followed by a second one published in 2005 (Buck et al., 2005) (cf. Figure 2). However, the lack of a digital representation or an open-access dataset confines data to a paper print, which is unsuitable for any further analytical work. We could have digitized from the contour lines, but the size of the images was already quite small (also note the blurriness of image 2a), moreover the scale and a reference point were not available, thus not lending themselves to a digitizing effort. Due to the lack of information on how they were created, lacking scale, reference points, and reference datum, and the overall poor image quality, a scanning-by-hand approach in all likelihood would introduce additional errors. Hence our need to recreate the bathymetry in digital format.

Nevertheless, these figures are valuable in that they show the general shape of the LE floor, which features two distinct bowls, one to the north of Isla de Cabritos and a shallower but larger one to the south of the island. LA, in contrast, has been researched much less over the years and as a result, there is no prior publication on its bathymetry. This lake features an elongated shape with steep edges on the north and south, bounded in three directions of N–S–E, and a broad shallow section on the west side as can be interpreted from Landsat images and the Shuttle Radar Topography Mission (SRTM) DEM.

3 | METHODOLOGY

3.1 | Data compilation and preparation

Our analysis is based on depth-surveying data acquired from several cruise expeditions in 2013 for both LA and LE (Piasecki & Moknatian, 2018; Piasecki et al., 2016). The data available from this source are single-beam soundings

into the lakes are of ephemeral nature (i.e. they will only carry water [runoff] after substantial storm events in the mountains). In addition, the river discharge is relatively small because of the porosity (karstic formations—Draper, Mann, & Lewis, 1994; Gonzalez, Domingo, Gonzalez, & Comarazamy, 2011) of the surrounding mountains that permits high infiltration rates (i.e. much of the precipitation in the mountains actually enters the lakes through subsurface flows with sediments already filtered out). Second, much of the slopes are made up of vegetated retaining soil and are also comprised of rocky substrate that (a) moves slowly and (b) does not have a lot of mobilizable small-size sediments. Third, recent work on the lakes involving coring (Sloan et al., 2017) showed that the amount of sediment added over decadal time scales is relatively small, suggesting that the lakes experience very low sedimentation rates, much below those reported by Sekellick et al. (2012) and Rahmani et al. (2018). We can also confirm from our own observations that the water in both lakes appeared quite transparent, with low turbidity. The final dataset has sufficiently high quality levels (class type 3: Reconnaissance) for our work (volume assessment), but would not correspond to a full lake bed survey needed for navigational chart quality-type bathymetric representations or targeting detailed bottom feature mappings. This would have required adherence to higher-level hydrographic data collection protocols. The single-beam soundings contained depth values of the lakes at the time of expedition with reference to the water surface as the vertical datum along the cruise track line. After the corrections, we used GIS software (ArcGIS 10.0) to convert all data points to WGS84 (horizontal) and EGM96 geoid (vertical) reference datums.

The spatial extent/cruise track line of the collection campaigns are presented in Figure 3 for reference. Soundings provided us with a total of 35,052 and 17,401 depth soundings for LE and LA, along 326 and 249 km of track line, respectively. The distance between the recorded points varied between one and a few hundred meters, with an average of 12.7 m (LE) and 14.4 m (LA). The distances between the transects were about 2 km (LE) and 1 km (LA) on average (with a minimum of 0.5 km and a maximum of 6 km in some places), over surface areas of 345.8 km² (LE) and 138.3 km² (LA).

In addition to the soundings, we used satellite images to extract and define the lakes' outlines over time, to establish a relationship of depth (or volume) as a function of surface area. Note that this approach only works for a lake that has shallow sections and sloping shorelines (i.e. a basin with perfectly vertical walls would not expand in surface area while adding volume, thus rendering the use of satellite image data impractical). The extracted outlines provided us with extra depth contour lines in time, to aid in defining and mapping the lakes' edges. These

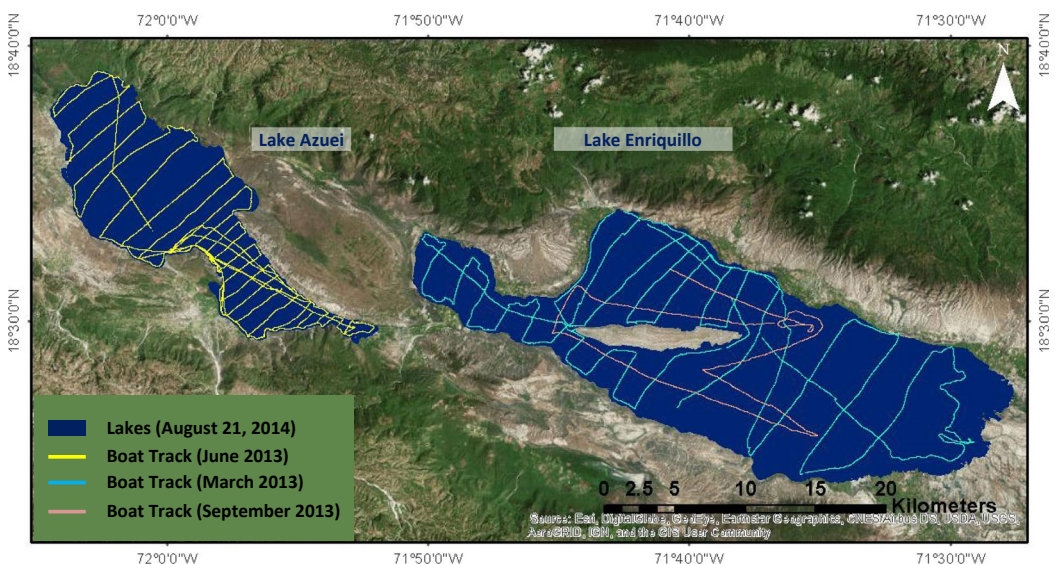


FIGURE 3 The spatial extent of the transects for Lakes Azuei and Enriquillo

contours filled the data gap along the shore at the time of survey (i.e. areas the survey vessel often could not get to). Toward this end, we performed an extensive search of the Landsat image archive reaching back 30 years (1984–2014) in order to identify cloud-free images of the lakes. Out of the data pool of 372 images, 16 were identified as suitable for both lakes. The Level 1 Terrain Corrected images were downloaded from the U.S. Geographical Survey (USGS) Global Visualization Viewer (<http://glovis.usgs.gov>) and the lakes' shorelines were later extracted, using the normalized difference water index (NDWI), following Moknatian, Piasecki, and Gonzalez (2017) from Landsat images of Hispaniola island and extracting the LA and LE extents for 1984 to 2014. The extracted outline for the year 2013, closest to the date of the sonar readings (more specifically, the images taken on March 27, 2013 [LE] and July 1, 2013 [LA]), was treated as the zero-depth line defining the boundaries of the lakes, thus allowing us to use lake outlines from preceding years as depth contours (during these years the lake level was much lower). We note that not all of the bathymetry survey points fell exactly inside the lakes' zero-depth outlines (shorelines) due to the resolution of the Landsat images (30×30 m). To address this issue, we removed another 560 (LE) and 463 (LA) points falling outside the shorelines, which make up about 2% of LE and 3% of LA total points of the bathymetric dataset, to produce consistent depths along the shoreline.

The corresponding depth values of each pre-2013 lake outline-based contour were assigned by masking the sounding points within a 2-m distance around and along the corresponding contour and averaging the depth values. Averaging helped in smoothing the differences between depth points and satellite-generated outlines that occasionally occurred. Again, these are the result of a relatively coarse 30-m resolution of the Landsat images which influences the lakes' outline spatial accuracy, resulting in more than one depth value along the lake outline. Figure 4 shows two examples of Landsat images taken 10 years apart (2003 and 2013) of the two lakes; note the dramatic difference in shoreline.

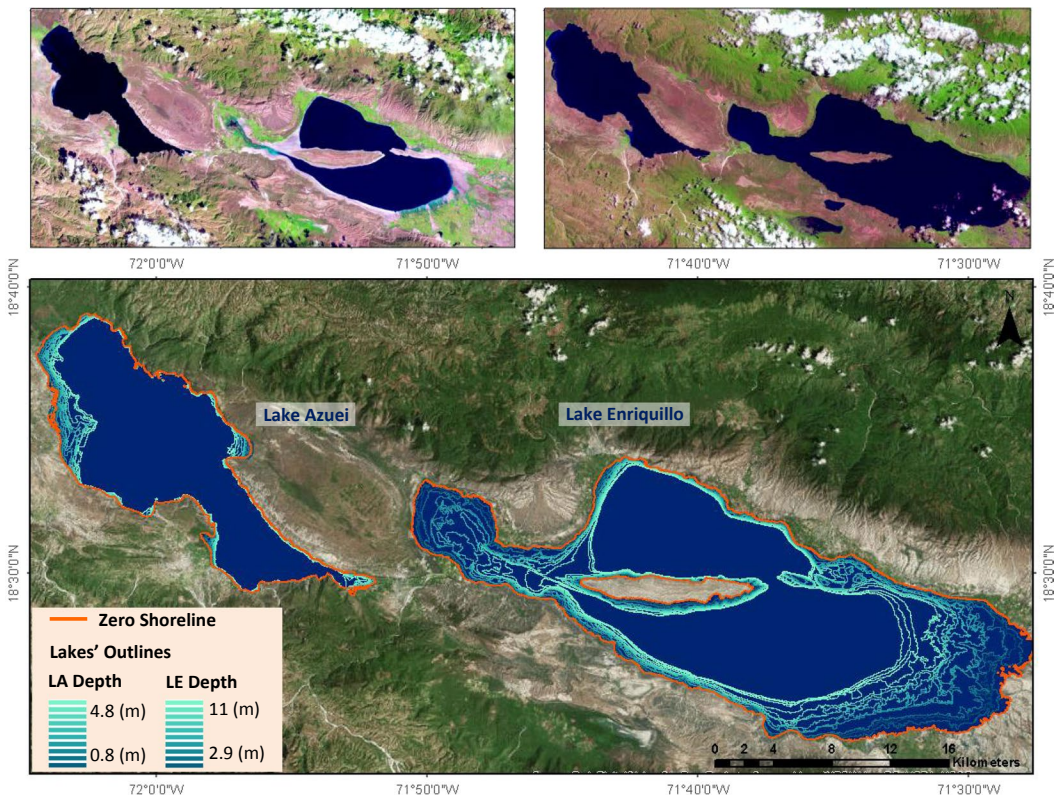


FIGURE 4 Landsat image taken on 2/12/2003 (top left), Landsat image taken on 7/25/2013 (top right), and extracted lakes' extents from Landsat images (bottom)

3.2 | Gridding algorithm/DBM creation algorithm

3.2.1 | Spatial interpolation

Among different interpolation methods, the ANUDEM method (hydrologically correct method) has shown its utility to produce more accurate products (Arun, 2013; Šiljeg, Lozić, & Šiljeg, 2015; Tan & Xu, 2014). Its use yields terrain that features both smooth and steep sections by defining the local slope and curvature (Hutchinson, 2011; Pavlova, 2017). Moreover, ANUDEM allows the use of different concurrent input data types, such as data points and contour lines. The method combines two algorithms of interpolation and drainage enforcement to produce a smooth surface from elevation datasets with respect to hydrologic correction. During the interpolation procedure, a regular grid for the smooth surface is built using the point or contour elevation data by employing an iterative finite difference technique based on minimizing a discretized rotation-invariant roughness penalty (Hutchinson, 1989). The drainage features of streamline, lake ridges, and channels are also incorporated in the interpolation as constraints, while sink points will be removed during the drainage enforcement process.

For a DTM to be considered a “best representation of a given terrain,” it should not only yield consistent elevation values but also accurately represent and be consistent with the slopes and curvatures of the real land surface (Kienzle, 2004). In ANUDEM, the curvature of fitted surfaces is controlled by user-defined roughness penalties, defined in terms of first and second-order partial derivatives of the fitted function, so that the DEM matches the sharp changes in terrain associated with peaks, streams, and ridges (Hutchinson, 2000).

ANUDEM introduces two parameters, namely the roughness penalty (RP) and profile curvature roughness penalty (PCRP). RP modifies the minimum curvature interpolation function by specifying the amount of potential to be added to the default total curvature penalty. This transformation helps the grid to fit to sharp changes in gradients, particularly at peaks. PCRP is defined as the curvature of the fitted surface in the downslope direction. This parameter is a locally adaptive factor that can be used to partly replace total curvature, helping the adjustment of the model to features such as rock outcrops, cliffs, and waterfalls (Hutchinson, 2000, 2011). Thus, the shape of the final product depends greatly on the proper selection of the RP and PCRP values (Hutchinson, 1989; Lewis, 2001). A combination of total and potential curvature has been found to yield better results when using point data rather than contour data. Therefore, RP values of zero and 0.5 are recommended when having contour and point data as main sources, respectively (Hutchinson, 1989, 2000, 2011). PCRP can range from zero to 0.9 depending on the characteristics of a given case study (Hutchinson, 2011). Improvement in ANUDEM results can be achieved by optimizing the interpolation algorithm parameters of RP and PCRP, output grid resolution, and number of iterations (Yang et al., 2007), or by employing auxiliary topographic data (Zheng et al., 2016). In this study, we chose a 30-m pixel resolution for the output grid in order to match the resolution of the surrounding SRTM DEM.

3.2.2 | Artifact detection

The highly anisotropic distribution of our survey soundings, especially in the center of the lakes, created large areas of no data. The distribution of these areas of no data created inside the smallest lake extent, in combination with the track lines, showed that 90% of LE had spaces of no data larger than 1.8 km², and 0.6 km² for LA, requiring approximately 2,000 (LE) and 700 (LA) grid cells for the smallest space to be filled when incorporating the required 30-m resolution of the output. The largest no-data areas for each lake were 13.7 km² (LE) and 14.16 km² (LA), respectively.

The areas with no data or sparse data are subject to artifact creation, introduced by the interpolation process (Arndt et al., 2013; Danielson et al., 2016; Moustier & Kleinrock, 1986). Once the raw gridded surface was created, we passed it through a thorough examination step to identify probable anomalous artifacts creation. We observed two sets of artifacts: (i) peak or sink shape patches (Figure 5a); and (ii) “rib” shape ridges (Figure 5b).

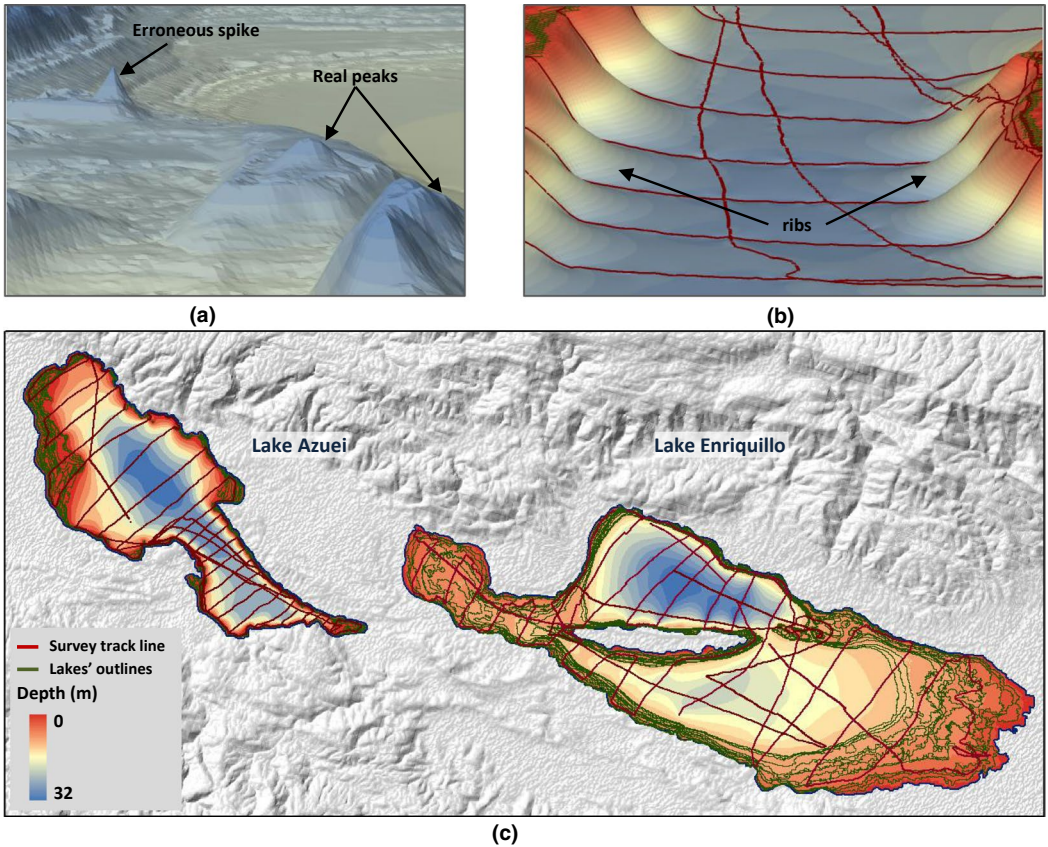


FIGURE 5 Raw surface gridded at 30-m resolution: (a) 3D view of spike shape area; (b) 3D view of “rib” shape area; and (c) overlaying the survey track lines, extracted lakes’ outlines, and raw models

Visualizing the gridded model together with the bathymetric source datasets (Figure 5c) showed that the peak or sink shape patches appeared mostly along the strip line between the smallest and largest lakes’ extent outlines, while “rib”-like features evolved in no-data areas. Further investigation of these anomalies showed that the peak/sink-shaped patches are either due to the existence of submerged objects such as structures or trees, or overlapping of the lake’s outlines resulting in an artifact. Removing these artifacts required some degree of care, during which we examined each suspected spot separately, trying to find images that were from a point in time when the area was not inundated. The points or line segments related to those areas were either kept (if they corresponded to an existing structure or small hills/islands) or eliminated from the dataset (if there was no indication of structure or object). Note that this “mowing” surveying pattern helps with the interpolation process, but does not cause any appreciable error in the final volume calculations.

Comparing the raw modeled surface with other references, and also inspecting the consistency in the occurrence of the “rib”-like anomalous areas in large patches appearing in no-data areas, suggested that these features did not represent the actual bed and are artifacts created by the interpolation algorithm. The profiles of the inward “rib” ridges running between the track lines were extracted and then compared to the slope profile of the closest track lines. It was noted that the slope of the bathymetry in between two adjacent track lines did not maintain the same elevation changes as the track lines would suggest, thus creating a smaller downhill slope causing “rib” shapes when viewed from the top.

To create the initial gridded surface, we used an RP value of 0.5, as suggested by Hutchinson (1988) for primary data types such as elevation points, and a PCRP value of zero (default). Subsequently, we modified these two

parameters to find optimum values that would result in the disappearance of the “rib” formations and thus correct slope and curvature. An RP value of zero (making the surface stiffer) seemed to result in some improvement for areas of gentle downslopes. Varying the PCR value, however, did not seem to yield a noticeable change in the bathymetry results. We thus kept it near the lower limit of zero, despite the results of other research efforts suggesting that the PCR value needs to be set higher in order to increase the slope of the profile (Yang, Van Niel, Mcvicar, Hutchinson, & Li, 2005; Yang et al., 2007). Changes in the RP and PCR parameters did not seem to work for the steep areas of the site. It is worth mentioning that the number of iterations of the interpolation process did not improve the results either.

The reasons why changes in the ANUDEM parameters did not yield satisfactory results were related to the density of the source points and the irregularity in distribution of the track lines. This also meant that the initial choice of a 30-m grid resolution proved unsuitable for the study area; in fact, the output grid resolution has a significant impact on ANUDEM performance. Thus, not being able to choose an optimum resolution for the outputs *a priori* introduced unwanted bias to the results. This was compounded by the highly irregular spatial distribution of sonar data over the lakes, with the distance between a target point and its four neighbors varying between 5 m (along the track) and 7 km (between two adjacent track lines).

If the best output resolution cannot be predetermined, some guidance has been provided that aids in selecting a good starting resolution based on both source data density and type of terrain. The optimal grid size is between the interval length of sample points and up to twice that when their spatial distribution is homogeneous. Otherwise, the DTM may be generated with insufficient information in one case or altered information in the other (William, Brian, Saul, & William, 1989). This means that the density of points in a unit surface (of the target resolution) should be between one and four. The data density investigation of input points for lakes showed a density of 101.7 and 126.3 points/km² for LE and LA, respectively. Considering the desired 30 × 30 m resolution of the bathymetry, the required density reduced to an average of 0.08 (LE: between 0 and 556 points/unit) and 0.1 (LA: between 0 and 144 points/unit) over the 30 × 30 m unit surface, while more than 94% of the grid cells contained no data at all. The density of points over the unit area of 30-m resolution was far less than the limit of 1–4 points/unit stated by William et al. (1989), thus indicating that the available source data density was actually not sufficient to generate an accurate 30 × 30 m cell size DBM.

3.2.3 | Introducing auxiliary contours using output resolution change

Because of the non-ideal spatial distribution of the input data, we had to develop a different strategy to utilize the sonar data. Kienzle (2004) showed that the optimum grid size for a DTM should be coarser when the profile and plan curvature of the terrain are the target features (Kienzle, 2004). In the ANUDEM algorithm, the grid generation starts from an initial coarse resolution, which is calculated from the average depth of all data values and which will then be interpolated onto a grid with a finer user-defined resolution (Hutchinson et al., 2011). The average depth values of data points for lakes were 11.22 m (LE) and 11.54 m (LA), which was finer than our desired 30 m grid size. This also explains why the ANUDEM algorithm could not eliminate the spurious ridges during its correction steps (i.e. the interpolation error propagates inside the no-data areas due to the data distribution—Brasington & Richards, 1998; Fisher & Tate, 2006).

In order to help eliminate the problem of erroneous slope and curvature, we decided to focus on the grid size and assess its effect on the “rib” creations. Arndt et al. (2013) suggested decreasing the resolution of the output surface in order to remove the artifacts and also improving the local curvature. However, decreasing the grid size results in losing detailed information and also the smooth lake outline. We repeatedly applied this process to both lakes, spanning a selection starting at 30-m grid (pixel) and going up to 1-km resolution.

As can be observed from Figure 6, the coarser the resolution the better (smoother) the contour-line presentation in terms of removing “rib”-like artifacts in areas of no data. A common method for void filling is to use a coarser grid size in areas with no data (Reuter, Nelson, & Jarvis, 2007; Robinson, Regetz, & Guralnick, 2014; Zheng et al., 2016). However, through the process of scale change, some details are lost, resulting in changes to DEM characteristics and

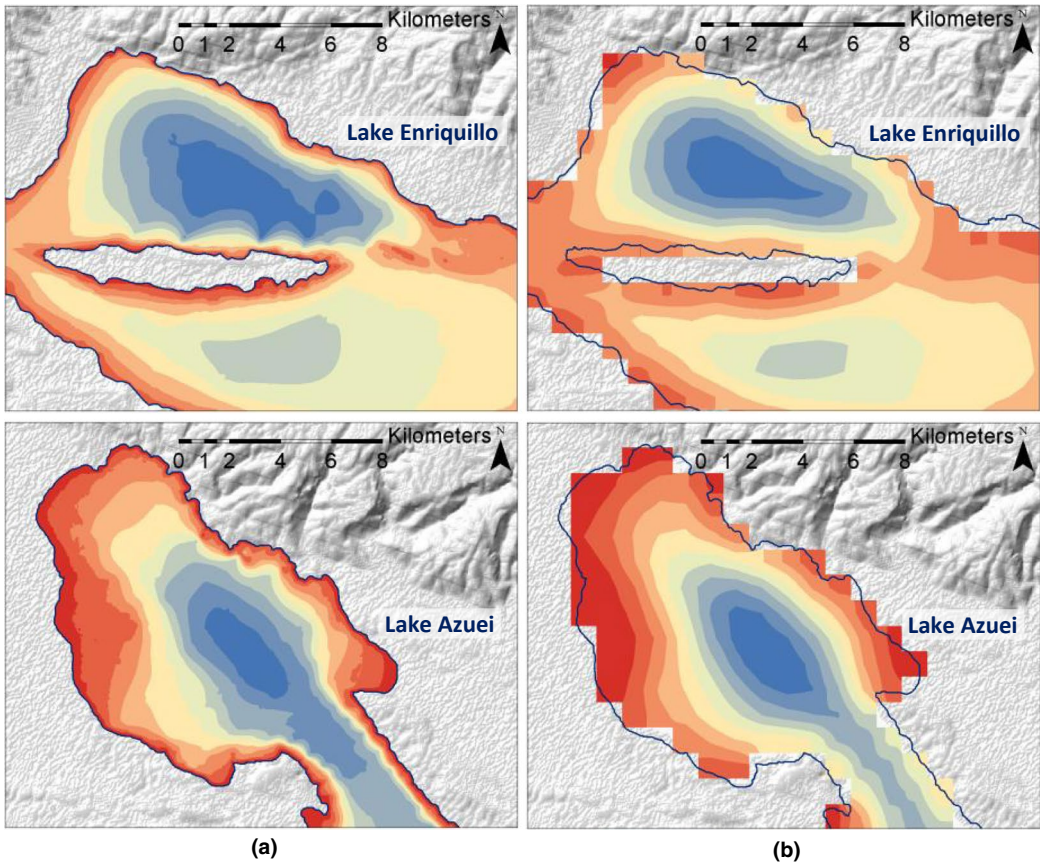


FIGURE 6 The effect of grid resolution change in the produced bathymetry (with adjusted RP and PCRPP): (a) 30-m resolution; and (b) 1-km resolution

consequently shapes of contour lines (Brasington, Rumsby, & McVey, 2000). Therefore, using topographic elements directly from low-resolution DEM as auxiliary input for void filling causes discrepancies between fine and coarse DEMs, a loss of vertical accuracy, and topological inconsistency of the final output DEM (Zheng et al., 2016). To overcome these problems, Zheng et al. (2016) proposed an improved ANUDEM technique to fill voids in a DEM. In this method, they used contour lines derived from multi-scale DEM (being coarse in areas of no data) as auxiliary input for ANUDEM. The information from the contours was corrected using the terrain topological structure before engaging the interpolation step. This method helped preserve the characteristics of the surface across different scales, recovering sharp terrain features in the resampled DEM, and reducing the inconsistency between the multi-scale data. As a result, the void-filled high-resolution DEM had higher vertical accuracy and their method was proved to generate high-quality auxiliary DEM data. Applying the same method, we decided to search for and identify the optimal grid size at which "rib"-like artifacts start to fade away in no-data areas, then extract extra contour lines for those areas, apply topographic correction, and subsequently insert them back into the bathymetry generation process as auxiliary contours. This is not a straightforward process, however, but requires iteration during which the number of contours and also their depth values need to be adjusted to match the depth soundings and lakes' outlines.

3.3 | Accuracy assessment

To assess the quality of a DTM, both the accuracy of the interpolated depth values and the shape reliability of the surface have to be validated (Desmet, 1997). Statistical methods applied to the modeled values and their

associated errors are helpful when the precision of the interpolation is the focus, while shape reliability can be assessed by examining the spatial distribution of the errors. We first tested the performance and accuracy of the interpolation using mean error (ME), mean absolute error (MAE), and root mean squared error (RMSE) indicators, showing the degree of bias, deviation of the bathymetry from the surveyed data, and overall accuracy of the produced bathymetry, respectively (Erdoğan, 2010):

$$ME = \frac{1}{n} \sum (\Delta D) \quad (1)$$

$$MAE = \frac{1}{n} \sum |\Delta D| \quad (2)$$

$$RMSE = \sqrt{\frac{1}{n} \sum (\Delta D)^2} \quad (3)$$

where ΔD represents the difference between overlapping datasets of the observed depth values from the input sources (sonar readings) and the interpolated/extracted depths from the bathymetry. For a DTM to be precise and unbiased, ME, MAE, and RMSE should be close to zero (Chen et al., 2016; Erdoğan, 2010). These indices are general indicators summarizing the algorithm performance in only a single value containing no detail on local errors. The two sets of observed depths and interpolated depths can be further analyzed using statistical tests to see whether the two datasets exhibit significant differences. The type of statistical test needed has to be chosen based on the statistical distribution of the depth values (parametric/non-parametric).

In order to investigate the randomness of the errors in the final product, we explored the statistical and spatial distribution of the residuals (ΔD). The statistical distribution of residuals shows the nature of the errors and can reveal whether the errors are following a distinct pattern, which is an indication of a systematic error produced by the interpolation method. In the same manner, identified patterns in the spatial distribution of the residuals indicate the distortion of the shape of a surface in the model. The two parameters which affect the spatial variability of the errors are landform type and interpolation method (Carlisle, 2005; Chaplot et al., 2006; Erdoğan, 2010). The correlation between these factors and the model residuals can be tested using diagnostic methods such as regression. Erdoğan (2010) used ordinary least squares regression and geographically weighted regression models to investigate the spatial relationship between the error/accuracy of three different interpolation algorithms and surface characteristics. Having identified a significant relationship between the two factors, he pointed out that studying this relationship would help determine the location and distribution of the measurement points, depending on the complexity of the topography.

4 | RESULTS AND DISCUSSION

To produce the final product, we selected an RP equal to zero and a PCRPF of 0.1 for both lakes. Successively varying the grid resolution, we noticed that at a resolution of 500 m the ribs faded away, while the contour lines were still smooth. At this resolution, the average density of data points increased to 20.46 (LE) and 24.25 (LA) points over the 0.5×0.5 km unit cell. We then extracted the 1-m contour lines located inside the smallest observed lake extent, inserted them into the ANUDEM algorithm, and modified them during each iteration until the desired 30-m grid-based bathymetry was obtained. Note that this process may not yield a 100% perfect representation of the actual lake beds, especially in the center/middle of the lakes, because the results are optimized in terms of minimizing the errors. Our stopping criterion was set as “less than 1%” change (i.e. if a change in grid size did not yield more than a 1% change in computed volume to the next, then we accepted the last grid size and its corresponding contour line distribution). The final generated bathymetry maps for both lakes with associated contour lines are presented in Figure 7a. Figure 7b also shows 3D views of the lakes.

While the final DBMs have less visible artifacts and also feature a smooth bathymetry, additional comparison with the original sounding datasets and also the remotely sensed lake shoreline is necessary to provide a post-processing accuracy assessment with respect to depth, volume, and lake shape.

4.1 | Depth accuracy

The accuracy was assessed by utilizing ME, MAE, and RMSE indices which are, alongside the maximum negative and positive errors, as well as the median value of error, shown in Table 1. The statistical comparison of the two datasets (i.e. of the observed depths from survey and RS-based outlines to corresponding extracted depth values from the generated DBMs) yielded non-significant differences. This comparison showed probability values (p values) larger than 0.05 (0.92 [soundings] and 0.87 [outlines] for LE and 0.49 [soundings] and 0.45 [outlines] for LA), meaning that the two sets have the same distribution with the same statistical parameters within the confidence level of 95% ($\alpha = 0.05$). Because the distributions of the observed and extracted depth values were not normal, we used the statistical non-parametric Wilcoxon rank sum test to compute p values.

The small values of the indices of ME, MAE, and RMSE for soundings and outlines suggest that the depth values are well preserved in the final DBMs. Moreover, the mean absolute percentage error (MAPE) yielded 16% (LA) and 12% (LE) when comparing the overlapping depth values of the final DBM and soundings. The occurrence of negative and positive values for maximum error for both lakes, however, suggested meters of difference in some places, which needed further investigation regarding the systematic error detection and shape reliability.

While the distribution of the residuals followed a normal distribution, indicating the random nature of the errors, Figure 8 shows that the larger errors are spatially concentrated at specific locations. Figure 8a shows

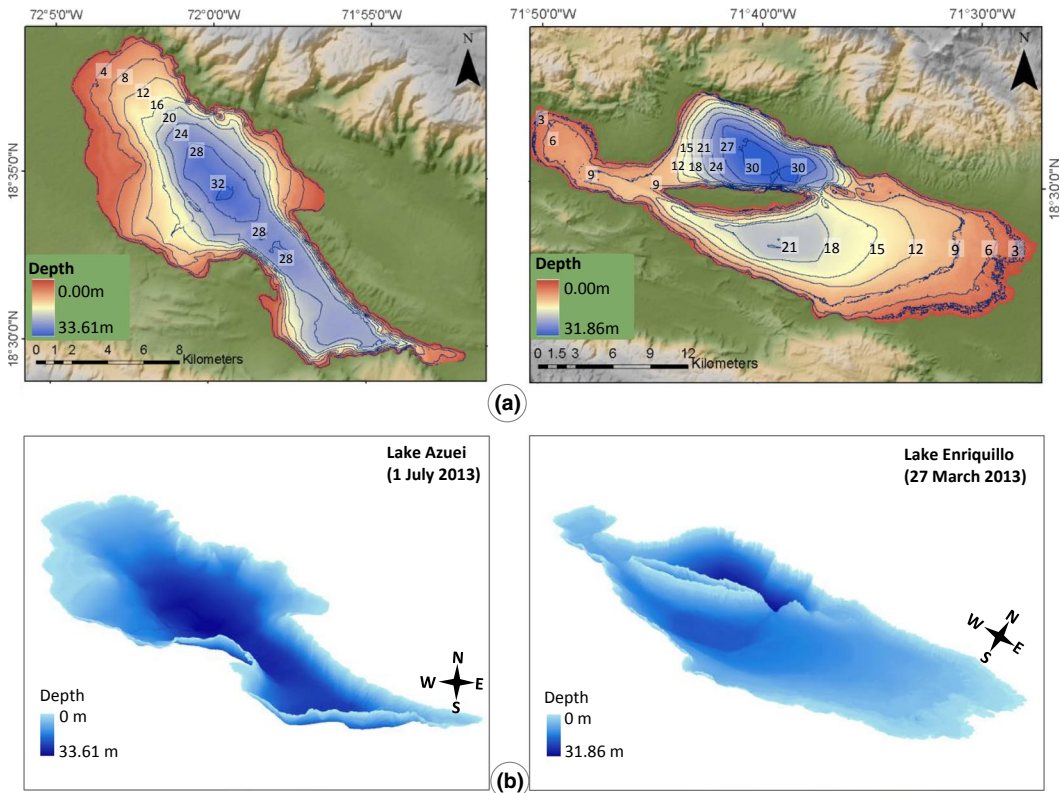


FIGURE 7 (a) Bathymetry presentation of Lake Azuei and Lake Enriquillo; and (b) 3D presentation of the bathymetry

TABLE 1 Accuracy parameters (m) resulting from the comparison of bathymetry depth with survey soundings and lakes' outlines

Lake	Source data	Max negative error	Max positive error	Median	ME (mean)	MAE	RMSE (SD)
Enriquillo	Soundings	-7.83	11.19	-0.0036	0.01	0.35	0.71
	Outlines	-2.61	4.26	-0.0139	-0.004	0.28	0.48
Azuei	Soundings	-4.98	10.30	-0.0007	0.07	0.50	0.96
	Outlines	-9.28	6.00	0.0254	0.03	0.56	0.88

that the lakes' edges were the predominant locations for overestimation (green color) and underestimation (red color), while for points in the lake interior the errors were much smaller (yellow color) and also more randomly distributed. We attribute this to two reasons: first, gentle slope regions (such as in the center) adjust much better to the input data; second, the edges had higher data density, were steeper, and also featured two different dataset sources with sometimes differing data values. Figure 8b presents an additional view of the magnitude of the errors (larger dots mean larger errors), which are clearly more prevalent along the edges, establishing the influence of the surface/terrain characteristics on the spatial variability of the residuals, resulting in systematic errors in the final bathymetry models.

Considering the fact that small depth values pair with either gentle or steep slopes along the edges, while interior points (especially in the bowl regions) have larger depths and smaller slopes, it is clear that the occurrence of errors and their signs are associated with the two surface characteristics of depth and slope. To find out how significant this relationship is, we carried out a regression test to evaluate the correlation of each of these parameters with actual and absolute error values. The regression analysis showed significant ($\alpha = 0.01$) effect of surface slope values on the actual error (the sign of the errors), while absolute errors (magnitude) were changing significantly corresponding to the lake depth, confirming the statements made above.

In addition to slope and depth, we also tested the characteristics of the survey soundings, to see if they contributed to the spatial consistency of the errors. These parameters included the density of the survey points, contour lines density, and types of input datasets (points/contour lines), none of which showed a statistically significant correlation with either the actual or the absolute errors.

However, contour line density, in combination with point density, gained statistical significance when correlated with the absolute error, even though it was small ($\alpha = 0.1$). The errors associated with contour line density added up with the errors associated with data point density and became significant when both densities for a specific area increased. The spatial distribution of systematic errors in the final model of the lakes resulted in surfaces with a more uniform curvature (i.e. making gentler slope areas steeper and steeper areas gentler), and thus contributed to a less favorable adjustment to the high slope and curvature changes along the edge.

4.2 | Volume accuracy

Since lake volume measurement is a key goal of our work, we examined how the quality of the lake bathymetry and lake shape would affect the volume. Toward this end, we calculated the volume accuracy along the track line. We converted the sonar-based depth soundings into grid cell depths and then computed the volume difference between these grid cells and the overlapping interpolated grid cells from the bathymetry model. While this could yield either positive or negative values, note that a zero difference does not mean identical lake shapes and depth, but rather that the overestimates and underestimates of the surface/depth cancel each other out (as depicted in Figure 9).

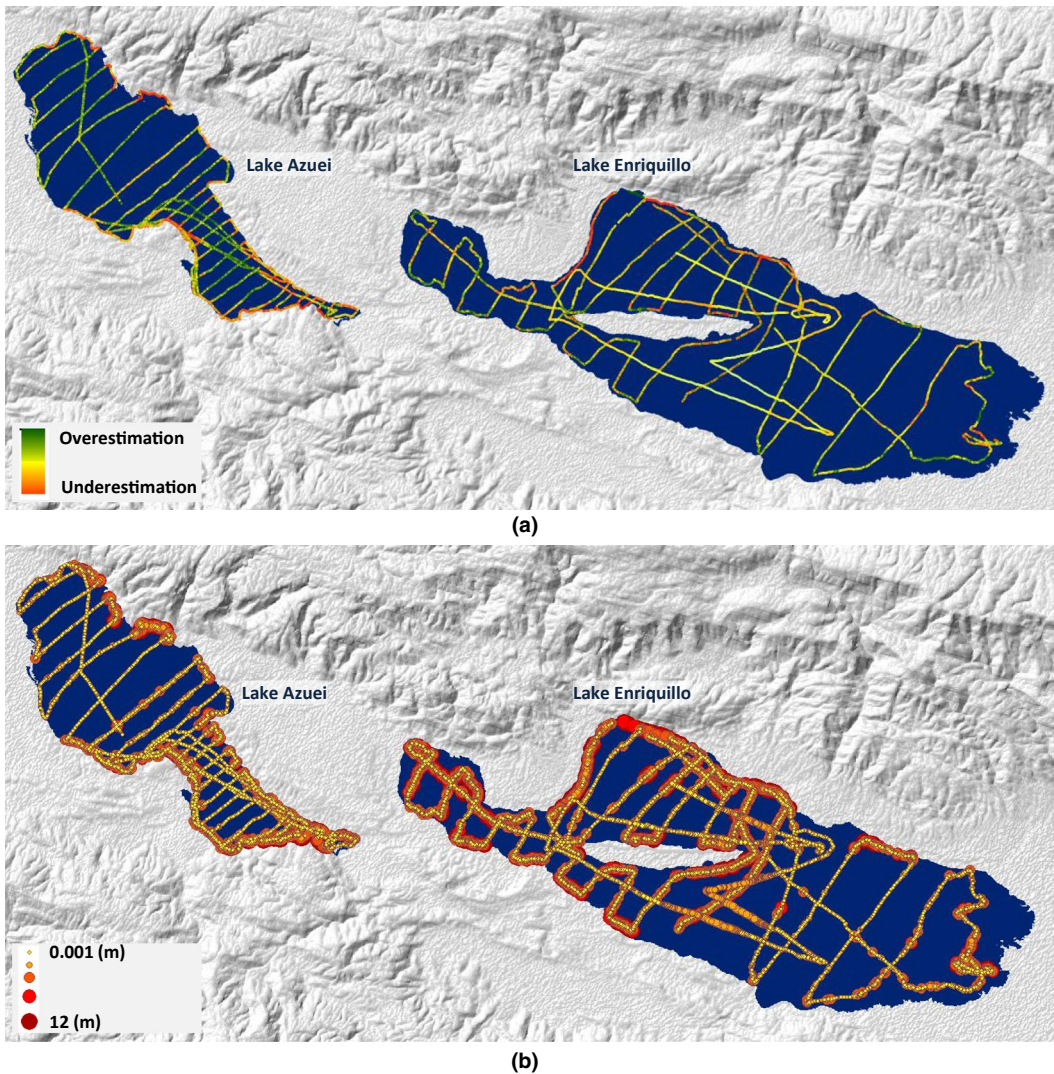


FIGURE 8 Spatial distribution of errors: (a) actual error (ΔD) (red color, underestimation; green color, overestimation); and (b) absolute error ($|\Delta D|$) (size, magnitude of the absolute error)

Negative maximum and positive maximum errors were computed for both lakes. The results ranged from -3 to $+8\%$ error in volume estimation for LA, while the corresponding errors for LE volume estimation were between -9 and $+6\%$. The average errors were 0.009% (LE) and 0.003% (LA), slightly underestimating the volume values. Note that the real/overall volume errors should be a little higher than the presented errors, since the interpolation worked better along the track line compared with using the spaces between.

As a final step, we compared the computed volumes of each lake based on the final bathymetry, and compared it to the raw and unimproved bathymetry to see how well the designed algorithm for eliminating the errors had worked. The result showed a 7.7% (LE) and a 4.2% (LA) difference, with the final product having the higher volume values. This means that retaining the “rib” shape features would have caused a significant underestimation of the lakes’ water volume and also highlights the need to go through quality control steps that remove these types of features to obtain both the true volume and the real shape of the bottom surface.

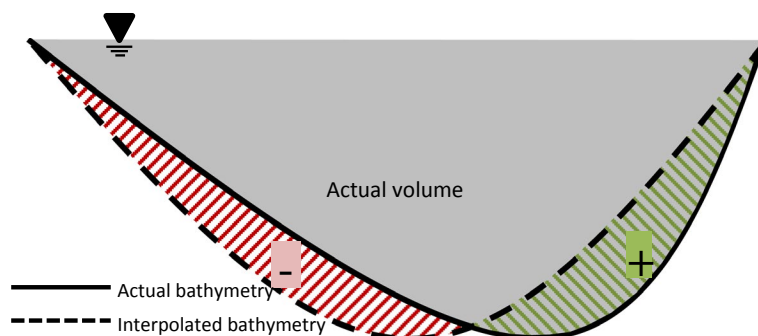


FIGURE 9 Actual and interpolated bathymetry scheme (the inverted triangle symbol represents water surface)

The final DBMs showed that at the time of the surveys (July 1, 2013), LA had a surface area of 137.84 km² (Landsat images with WGS84/UTM zone 19N projection). The lake had an elongated bowl shape with a slope of less than 0.5% in the center and on the west shallow edges and up to 10.53% in the southern part of the lake. The mean value of the slope was 1.05% with a standard deviation of 1.23%, while the volume value derived from the bathymetry was 1.997 km³. LE was characterized by slopes ranging between 0.001 and 6.63% (mean: 0.66%, SD: 0.8%). The surface area of LE was 345.85 km² with a corresponding volume of 3.8 km³ derived from the bathymetry model (March 27, 2013). Both lakes have a similar maximum depth value of a little more than 30 m (31.86 m [LE], 33.61 m [LA]).

5 | CONCLUSIONS

Based on sonar depth data collected during a campaign in 2013, as well as a dataset of lake outline extractions from Landsat imagery, we developed DBMs of Lakes Enriquillo and Azuei, using the ANUDEM module. The use of the ANUDEM method proved to be a suitable approach for developing accurate DBMs by utilizing the algorithm's ability to permit different types of datasets, such as point clouds and polygons. Analyzing early DBMs created with ANUDEM showed how the density and spatial distribution of the input data, and the required DTM resolution, affected the result of the interpolation, resulting in the creation of artifacts along the edges of the lakes inside no-data areas. To eliminate the artifacts, we designed an iterative workflow to improve the accuracy of the lake DBMs by introducing topographically corrected auxiliary contour lines derived from low-resolution models. These auxiliary contour lines act as "guidelines" during the ANUDEM run, improving the DBM model generation when switching to higher-resolution grids. The algorithm we use is a combination of workflows in ArcGIS Model Builder, MATLAB codes, and several manual editing efforts.

We introduced statistical concepts to assess the quality of each newly created DBM by comparing newly created DBMs with those created without any improvement steps. The outcome showed MAE of less than 0.5 m for both lakes' depth representations and a 7.7% (LE)/4.2% (LA) improvement in volume estimation by removing inward "rib"-shaped artifacts. We also observed systematic patterns in the spatial error distribution. Regression tests showed that the pattern is correlated with the complexity of the topography/curvature along the edges of the lakes and the inconsistency between the input data sources. Although it was expected that the high density of data would help increase the accuracy of the final model, it was observed that the inconsistency between the values of different data sources introduced errors to the DBMs.

Due to the existence of these errors, the final DBMs were more uniformly bowl-shaped with smoothed curvature/slope differences. Despite this shape distortion, the accuracy analysis carried out for volume estimation

resulted in less than 10% absolute errors and less than 0.01% average error for overlapping areas of the model and the underlying soundings. Based on these results, we conclude that the precision and accuracy of a DBM can be increased if one deploys error minimization techniques in addition to controlling the input data by designing the proper density and distribution pattern for track lines. These should be based on the terrain morphology and required map resolution, as well as *a priori* assessment of the different data types, subjecting them to a quality assessment procedure before inserting them into the ANUDEM algorithm.

To our knowledge, the developed DBMs for both lakes are the first publication of a digital representation of the lakes and can be requested from the authors of this article.

ACKNOWLEDGMENTS

This research was supported by the National Science Foundation through Grant Nos. 1264466 and 1513512. We also acknowledge support from the Grove School of Engineering at the City College of New York. This work would not have been possible without the involvement of numerous students (Paul Celicourt, Joseph Cleto, Ambar Mesa) and researchers (Yolanda Leon at INTEC, Lavaud Vernet, and Steffen Schneider). The data for this research can either be requested from the corresponding author, Dr. Michael Piasecki (michael.piasecki@gmail.com), or be found in the City University of New York Academic Works public library installation at <https://academicworks.cuny.edu>.

CONFLICT OF INTEREST

The authors declare no conflict of interest.

ORCID

Michael Piasecki  <https://orcid.org/0000-0002-4047-8063>

REFERENCES

- Aguilar, F. J., Agüera, F., Aguilar, M. A., & Carvajal, F. (2005). Effects of terrain morphology, sampling density, and interpolation methods on grid DEM accuracy. *Photogrammetric Engineering & Remote Sensing*, 71(7), 805–816.
- Araguás Araguás, L., Mchelen, C., Garcia, A., Medina, J., & Febrillet, J. (1995). *Estudio de la Dinamica del Lago Enriquillo: Segundo informe de avance* (Project DOM/8/006). Vienna, Austria: International Atomic Energy Agency.
- Arndt, J. E., Schenke, H. W., Jakobsson, M., Nitsche, F. O., Buys, G., Goleby, B., ... Wigley, R. (2013). The international bathymetric chart of the Southern Ocean (IBCSO) version 1.0: A new bathymetric compilation covering circum-Antarctic waters. *Geophysical Research Letters*, 40(12), 3111–3117.
- Arun, P. V. (2013). A comparative analysis of different DEM interpolation methods. *Egyptian Journal of Remote Sensing & Space Science*, 16(2), 133–139.
- Bates, P. D., & De Roo, A. P. J. (2000). A simple raster-based model for flood inundation simulation. *Journal of Hydrology*, 236(1&2), 54–77.
- Benson, L. V., & Paillet, F. L. (1989). The use of total lake-surface area as an indicator of climatic change: Examples from the Lahontan basin. *Quaternary Research*, 32(3), 262–275.
- Bhattarai, R., & Dutta, D. (2007). Estimation of soil erosion and sediment yield using GIS at catchment scale. *Water Resources Management*, 21(10), 1635–1647.
- Brasington, J., & Richards, K. (1998). Interactions between model predictions, parameters and DTM scales for TOPMODEL. *Computers & Geosciences*, 24(4), 299–314.
- Brasington, J., Rumsby, B. T., & McVey, R. A. (2000). Monitoring and modelling morphological change in a braided gravel-bed river using high resolution GPS-based survey. *Earth Surface Processes & Landforms*, 25(9), 973–990.
- Buck, D. G., Brenner, M., Hodell, D. A., Curtis, J. H., Martin, J. B., & Pagani, M. (2005). Physical and chemical properties of hypersaline Lago Enriquillo, Dominican Republic. *Verhandlungen Des Internationalen Verein Limnologie*, 29(1), 1–7.
- Carlisle, B. H. (2005). Modelling the spatial distribution of DEM error. *Transactions in GIS*, 9(4), 521–540.

- Chaplot, V., Darboux, F., Bourennane, H., Legu dois, S., Silvera, N., & Phachomphon, K. (2006). Accuracy of interpolation techniques for the derivation of digital elevation models in relation to landform types and data density. *Geomorphology*, 77(1&2), 126–141.
- Chen, Y., Shan, X., Jin, X., Yang, T., Dai, F., & Yang, D. (2016). A comparative study of spatial interpolation methods for determining fishery resources density in the Yellow Sea. *Acta Oceanologica Sinica*, 35(12), 65–72.
- Daniell, J. J. (2008). Development of a bathymetric grid for the Gulf of Papua and adjacent areas: A note describing its development. *Journal of Geophysical Research: Earth Surface*, 113(1), 1–8.
- Danielson, J. J., Poppenga, S. K., Brock, J. C., Evans, G. A., Tyler, D. J., Gesch, D. B., ... Barras, J. A. (2016). Topobathymetric elevation model development using a new methodology: Coastal National Elevation Database. *Journal of Coastal Research*, 76, 75–89.
- Daut, G., M usbacher, R., Baade, J., Gleixner, G., Kroemer, E., M ugler, I., ... Zhu, L. (2010). Late Quaternary hydrological changes inferred from lake level fluctuations of Nam Co (Tibetan Plateau, China). *Quaternary International*, 218(1&2), 86–93.
- De Araujo, J. C., Fortes, I. S. F. C., Duarte, F. C., Pereira, B. S. B., Santos, E. E. D. S., & Seoane, J. C. S. (2016). Low-cost bathymetric survey for marine protected areas: Coral reefs and coastal islands. In *Proceedings of the 2015 IEEE/OES Acoustics in Underwater Geosciences Symposium*. Rio de Janeiro, Brazil.
- Desmet, P. J. J. (1997). Effects of interpolation errors on the analysis of DEMs. *Earth Surface Processes & Landforms*, 22(6), 563–580.
- Dozier, J., & Frew, J. (1990). Rapid calculation of terrain parameters for radiation modeling from digital elevation data. *IEEE Transactions on Geoscience & Remote Sensing*, 28(5), 963–969.
- Draper, G., Mann, P., & Lewis, J. (1994). Hispaniola. In S. K. Donovan & T. A. Jackson (Eds.), *Caribbean geology* (pp. 129–150). Kingston, Jamaica: University of the West Indies Publishers' Association.
- Erdođan, S. (2010). Modelling the spatial distribution of DEM error with geographically weighted regression: An experimental study. *Computers & Geosciences*, 36(1), 34–43.
- Fisher, P. F., & Tate, N. J. (2006). Causes and consequences of error in digital elevation models. *Progress in Physical Geography*, 30(4), 467–489.
- Fretwell, P. T., Tate, A. J., Deen, T. J., & Belchier, M. (2009). Compilation of a new bathymetric dataset of South Georgia. *Antarctic Science*, 21(2), 171.
- Gold, C. M., & Condal, A. R. (1995). A spatial data structure integrating GIS and simulation in a marine environment. *Marine Geodesy*, 18(3), 213–228.
- Gong, J., Zhilin, L., Zhu, Q., Sui, H., & Zhou, Y. (2000). Effects of various factors on the accuracy of DEMs: An intensive experimental investigation. *Photogrammetric Engineering & Remote Sensing*, 66(9), 1113–1117.
- Gonzalez, R., Domingo, R.-B., Gonzalez, J., & Comarazamy, D. (2011). *Estudio Hidrogeologico de la Zona del Lago Enriquillo, Determinacion de las Causas del Aumento de Nivel de sus Aguas e Intervenciones Requeridas para su Control* (Informe N.2 de Avnace del Protecto). Santo Domingo, Dominican Republic: INDRHI.
- Gumus, K., & Sen, A. (2013). Comparison of spatial interpolation methods and multi-layer neural networks for different point distributions on a digital elevation model. *Geodetski Vestnik*, 57(3), 523–543.
- Haile, A., & Rientjes, T. (2005). Effects of LiDAR DEM resolution in flood modelling: A model sensitivity study for the city of Tegucigalpa, Honduras. In *Proceedings of the ISPRS WG III/3, III/4, V/3 Laser Scanning Workshop* (pp. 168–173). Enschede, the Netherlands: ISPRS.
- Hillenbrand, C., Trathan, P. N., Arndt, J. E., & Kuhn, G. (2014). A new bathymetric compilation for the South Orkney Islands region, Antarctic Peninsula (49–39 W to 64–59 S): Insights into the glacial development of the continental shelf. *Geochemistry, Geophysics, Geosystems*, 15, 2494–2514.
- Hradilek, V., Bařta, P., Vizina, ř., M aca, P., & Pech, P. (2015). Verification of remote sensing data for measuring bathymetry on small water reservoirs. In *Proceedings of the 15th International Surveying, Geology Mining and Ecological Management GeoConference* (pp. 1219–1226). Albena, Bulgaria: SGEM.
- Hutchinson, M. F. (1989). A new procedure for gridding elevation and stream line data with automatic removal of spurious pits. *Journal of Hydrology*, 106(3&4), 211–232.
- Hutchinson, M. F. (2000). Optimising the degree of data smoothing for locally adaptive finite element bivariate smoothing splines. *ANZIAM Journal*, 42, 774–796.
- Hutchinson, M. F. (2011). *ANUDEM Version 5.3 User Guide*. Canberra, ACT, Australia: Fenner School of Environment and Society, Australian National University.
- Hutchinson, M., Xu, T., & Stein, J. (2011). Recent progress in the ANUDEM elevation gridding procedure. In *Proceedings of the 5th International Geomorphometry Symposium* (pp. 19–22). Redlands, CA, USA.
- Ikechukwu, M. N., Ebinne, E., Idorenyin, U., & Raphael, N. I. (2017). Accuracy assessment and comparative analysis of IDW, spline and kriging in spatial interpolation of landform (topography): An experimental study. *Journal of Geographic Information System*, 9(3), 354–371.

- Jones, R. (2002). Algorithms for using a DEM for mapping catchment areas of stream sediment samples. *Computers & Geosciences*, 28(9), 1051–1060.
- Kienzle, S. (2004). The effect of DEM raster resolution on first order, second order and compound terrain derivatives. *Transactions in GIS*, 8(1), 83–111.
- Leon, J. X., & Cohen, T. J. (2012). An improved bathymetric model for the modern and palaeo Lake Eyre. *Geomorphology*, 173&174, 69–79.
- Lewis, A. (2001). *Great Barrier Reef depth and elevation model: GBRDEM* (Technical Report No. 33). Townsville, QLD, Australia: CRC Reef Research Centre.
- Li, Z., Zhu, Q., & Gold, C. (2005). *Digital terrain modeling: Principles and methodology*. Boca Raton, FL: CRC Press.
- Lu, D., Li, G., Valladares, G., & Batistella, M. (2004). Mapping soil erosion risk in Rondonia, Brazilian Amazonia: Using RUSLE, remote sensing and GIS. *Land Degradation & Development*, 15, 499–512.
- Mason, I. M., Guzkowska, M. A. J., Rapley, C. G., & Street-Perrott, F. A. (1994). The response of lake levels and areas to climatic change. *Climatic Change*, 27(2), 161–197.
- Moknatian, M., Piasecki, M., & Gonzalez, J. (2017). Development of geospatial and temporal characteristics for Hispaniola's Lake Azuei and Enriquillo using Landsat imagery. *Remote Sensing*, 9(6), 510.
- Moustier, C. De, & Kleinrock, M. C. (1986). Bathymetric artifacts in Sea Beam data: How to recognize them and what causes them. *Journal of Geophysical Research*, 91(5), 3407–3424.
- Nolan, M., & Brigham-Grette, J. (2006). Basic hydrology, limnology, and meteorology of modern Lake El'gygytgyn, Siberia. *Journal of Paleolimnology*, 37(1), 170–235.
- Parker, B., Milbert, D., Wilson, R., Bailey, J., & Gesch, D. (2001). Blending bathymetry with topography: The Tampa Bay demonstration project. In *Proceedings of the 2001 U.S. Hydrographic Conference*. Norfolk, VA.
- Pavlova, A. I. (2017). Analysis of elevation interpolation methods for creating digital elevation models. *Optoelectronics, Instrumentation & Data Processing*, 53(2), 171–177.
- Piasecki, M., & Moknatian, M. (2018). *Bathymetry data for Lakes Azuei and Enriquillo*. New York, NY: CUNY Academic Works.
- Piasecki, M., Moknatian, M., Moshary, F., Cleto, J., Leon, Y., Gonzalez, J., & Comarazamy, D. (2016). *Bathymetric survey for Lakes Azuei and Enriquillo, Hispaniola*. New York, NY: CUNY Academic Works.
- Popielarczyk, D., & Templin, T. (2014). Application of integrated GNSS/hydroacoustic measurements and GIS geodata-base models for bottom analysis of Lake Hancza: The deepest inland reservoir in Poland. *Pure & Applied Geophysics*, 171(6), 997–1011.
- Rahmani, V., Kastens, J., de Noyelles, F., Jakubauskas, M., Martinko, E., Huggins, D., ... Blackwood, A. (2018). Examining storage capacity loss and sedimentation rate of large reservoirs in the central U.S. Great Plains. *Water*, 10(2), 190.
- Reuter, H. I., Nelson, A., & Jarvis, A. (2007). An evaluation of void-filling interpolation methods for SRTM data. *International Journal of Geographical Information Science*, 21(9), 983–1008.
- Robinson, N., Regetz, J., & Guralnick, R. P. (2014). EarthEnv-DEM90: A nearly-global, void-free, multiscale smoothed, 90m digital elevation model from fused ASTER and SRTM data. *ISPRS Journal of Photogrammetry & Remote Sensing*, 87, 57–67.
- Sekellick, A., Banks, W., & Myers, M. (2012). *Water Volume and Sediment Volume and Density in Lake Lingaore between Boyers Mill Road Bridge and Bens Branch, Frederick County, Maryland* (Scientific Investigations Report 2013-5082). Washington, D.C.: U.S. Geological Survey.
- Šiljeg, A., Lozić, S., & Šiljeg, S. (2015). A comparison of interpolation methods on the basis of data obtained from a bathymetric survey of Lake Vrana, Croatia. *Hydrology & Earth System Sciences*, 19(8), 3653–3666.
- Sloan, H., Cormier, M.-H., Brown, B., Boisson, D., Guerrier, K., Hearn, C. K., ... Wattus, N. J. (2017). Sub bottom seismic profiling survey of Lake Azuei, Haiti: Seismic signature of paleo shorelines in a transpressional environment and possible tectonic implications. In *Proceedings of the Fall Meeting of the American Geophysical Union*. San Francisco, CA: AGU.
- Tan, Q., & Xu, X. (2014). Comparative analysis of spatial interpolation methods: An experimental study. *Sensors & Transducers*, 165(2), 155–163.
- Vogt, J. V., Colombo, R., & Bertolo, F. (2003). Deriving drainage networks and catchment boundaries: A new methodology combining digital elevation data and environmental characteristics. *Geomorphology*, 53(3&4), 281–298.
- Whiteway, T. G. (2009). *Australian bathymetry and topography grid* (Record 2009/21). Canberra, ACT, Australia: Geoscience Australia.
- William, H. P., Brian, P. F., Saul, A. T., & William, T. V. (1989). *Numerical recipes: The art of scientific computing* (Fortran version). Cambridge, UK: Cambridge University Press.
- Winstral, A., & Marks, D. (2002). Simulating wind fields and snow redistribution using terrain-based parameters to model snow accumulation and melt over a semi-arid mountain catchment. *Hydrological Processes*, 16(18), 3585–3603.

- Yang, Q. K., McVicar, T. R., Van Niel, T. G., Hutchinson, M. F., Li, L. T., & Zhang, X. P. (2007). Improving a digital elevation model by reducing source data errors and optimising interpolation algorithm parameters: An example in the Loess Plateau, China. *International Journal of Applied Earth Observation & Geoinformation*, 9(3), 235–246.
- Yang, Q., Van Niel, T. G., McVicar, T. R., Hutchinson, M. F., & Li, L. (2005). *Developing a Digital Elevation Model using ANUDEM for the Coarse Sandy Hilly Catchments of the Loess Plateau, China*. Canberra, Australia: CSIRO Land and Water Technical Report 7/05.
- Zerger, A., & Wealands, S. (2004). Beyond modelling: Linking models with GIS for flood risk management. *Natural Hazards*, 33(2), 191–208.
- Zheng, X., Xiong, H., Yue, L., & Gong, J. (2016). An improved ANUDEM method combining topographic correction and DEM interpolation. *Geocarto International*, 31(5), 492–505.
- Zimmerman, D., Pavlik, C., Ruggles, A., & Armstrong, M. P. (1999). An experimental comparison of ordinary and universal kriging and inverse distance weighting. *Mathematical Geology*, 31(4), 375–390.

How to cite this article: Moknatian M, Piasecki M, Moshary F, Gonzalez J. Development of digital bathymetry maps for Lakes Azuei and Enriquillo using sonar and remote sensing techniques. *Transactions in GIS*. 2019;00:1–19. <https://doi.org/10.1111/tgis.12532>